The Journal of Toxicological Sciences (J. Toxicol. Sci.)
Vol.50, No.4, 187-198, 2025

Original Article

Effect of the barrier function of stratum corneum and viable epidermis and dermis on the skin concentration of topically applied chemicals

Hiroaki Todo[1], Takeshi Oshizaka[2], Syuuhei Komatsu[1] and Kenji Sugibayashi[2]

[1]Faculty of Pharmacy and Pharmaceutical Sciences, Josai University, 1-1 Keyakidai, Sakado 350-0295, Japan
[2]Faculty of Pharmaceutical Sciences, Josai International University, 1 Gumyo, Togane, Chiba 283-8555, Japan

(Received October 16, 2024; Accepted February 10, 2025)

ABSTRACT — Three-dimensional cultured skin (3D skin) models have been utilized for *in vitro* skin permeation tests to evaluate the skin permeation rate and local effects (efficacy and toxicity) of applied chemicals, particularly from the perspective of the 3Rs (reduction, replacement, refinement) approach. The steady-state concentration of applied chemicals at different depths in the viable epidermis and dermis (*VED*) is affected by their skin permeation parameters, such as permeability coefficient (K_p) and partition coefficient (K) from the donor solution to the skin of the chemicals. In the present study, the steady-state concentration of chemicals in the *VED* of EpiDerm 606X (EpiDerm) as representative of a 3D skin model were compared with hairless rat skin. The *VED* concentrations of chemicals in EpiDerm were higher than those in hairless rat skin when a model hydrophilic compound, antipyrine, and a model lipophilic compound, flurbiprofen, were applied, suggesting that the barrier functions of the *VED* against the whole skin were higher in EpiDerm than in hairless rat skin. When an ester compound, ethyl nicotinate, was applied, the *VED* concentration of nicotinic acid, a metabolite of ethyl nicotinate, was lower in EpiDerm than in hairless rat skin. These differences in the *VED* concentrations of applied chemicals might be related to false-positives and -negatives of topical effects evaluated with 3D skin models. It is important to pay particular attention to differences in *VED* concentration in 3D skin models and real skin when evaluating local efficacy and toxicity using 3D skin models.

Key words: Three-dimensional cultured skin model, False negative, False positive, Barrier function, Skin permeation

INTRODUCTION

Recently, many *in vitro* approaches have been constructed to predict human risk assessment for raw materials and chemicals (Punt *et al*., 2020; Stucki *et al*., 2022). In particular, skin irritation, skin corrosion, sensitization, and photosensitization tests are a requirement for the evaluation of novel active ingredients for topical pharmaceutical and cosmetic use (Filaire *et al*., 2022; Zhao *et al*., 2023). In addition, *in vitro* approaches such as three-dimensional skin (3D skin) models have increasingly been used as a tool to evaluate the skin permeation and local effects of applied ingredients (Filaire *et al*., 2022). *In vitro* experiments with 3D skin models have the advantage of low variation in skin permeation profiles of chemicals compared with excised human skin (Sekiguchi *et al*., 2023). In addition, the expression of metabolic enzymes such as cytochrome P450 in 3D cultured skin models has been reported (Gibbs *et al*., 2007), thereby detecting metabolites of applied chemicals in the 3D skin model.

In vitro skin permeation tests provide permeation parameters such as the steady-state skin permeation rate of chemicals, J_{ss}. J_{ss} is expressed using Fick's first law of diffusion as follows:

$$J_{ss} = \frac{C_v \cdot D \cdot K}{L} \quad (1)$$

where C_v, K, D, and L are the applied chemical concentration, partition coefficients of the chemical into the skin barrier, diffusion coefficient of the chemical in the skin barrier, and the skin barrier thickness, respectively.

Correspondence: Hiroaki Todo (E-mail: ht-todo@josai.ac.jp)

This equation shows that the skin permeation of chemicals increases with increases in K and D and decreases in L value (equating to thinner skin barrier). Potts and Guy (1992) and Mitragotri *et al*. (2011) reported *in silico* models to predict the skin permeation of chemicals through native skin using the molecular weight (*M.W.*) and lipophilicity (logarithm of *n*-octanol/water coefficients, log $K_{o/w}$) of chemicals as input descriptors. There is a linear relationship between the log $K_{o/w}$ of chemicals and the K value in the skin, so it is desirable that the K value in 3D skin models should increase with an increase in the log $K_{o/w}$ value, as observed for human skin.

The skin membrane simply consists of two layers: the stratum corneum (*SC*) as a lipophilic layer and the viable epidermis and dermis (*VED*) as a hydrophilic layer. The *SC* is a strong barrier against hydrophilic drugs, whereas the *VED* provides a barrier against lipophilic drugs. Therefore, skin thickness is a crucial point in evaluating the risk assessment of the skin exposure of chemicals (Pirot *et al*., 1997). Takeuchi *et al*. (2012) and Yamaguchi *et al*. (2008) reported that the permeability coefficients of chemicals (K_p) through full-thickness skin were affected by the *VED* thickness, especially for lipophilic chemicals. K_p is expressed in a skin resistance model with R_{SC} and R_{VED}, which are calculated using the reciprocal of K_p through the *SC* (K_{p_SC}) and the *VED* (K_{p_VED}), respectively, as follows:

$$R = R_{SC} + R_{VED} \quad \text{or} \quad {}^{1}/_{K_p} = {}^{1}/_{K_{P\_SC}} + {}^{1}/_{K_{P\_VED}} \qquad (2)$$

In our previous study, we indicated that the steady-state skin concentration of chemicals was calculated using skin permeation parameters, which were obtained from the skin permeation profile from an *in vitro* skin permeation test (Sugibayashi *et al*., 2010). Briefly, because the permeation resistance of the chemicals can be represented as in the electric circuit, the ratio of the line segment ab against bc at x=*L*sc in the Fig. 1 should be the ratio of R_{SC} against R_{VED}. Thus, the chemical concentration at point b, C_b, can be represented by:

$$C_b = K_{SC} \cdot C_v \cdot R_{VED}/R \ \text{ or } \ K_{SC} \cdot C_v \cdot K_p/K_{p\_VED} \qquad (3)$$

Where C_v is the applied concentration of the chemical.

Because the partition coefficient of chemicals from the *SC* to *VED* is represented as K_{VED}/K_{SC}, the chemical concentration at point c, C_c, can be represented by

$$C_c = K_{SC} \cdot C_v \cdot K_p/K_{p\_VED} \cdot K_{VED}/K_{SC} \qquad (4)$$

A steady-state skin concentration in the *VED* layer can be theoretically represented by the triangle area shown in the region of Fig. 1 (i) with a skin resistance model (eq. 5).

$$C_{VED} = \frac{K_{VED} \cdot C_v \cdot K_p/K_{p\_VED}}{2} \qquad (5)$$

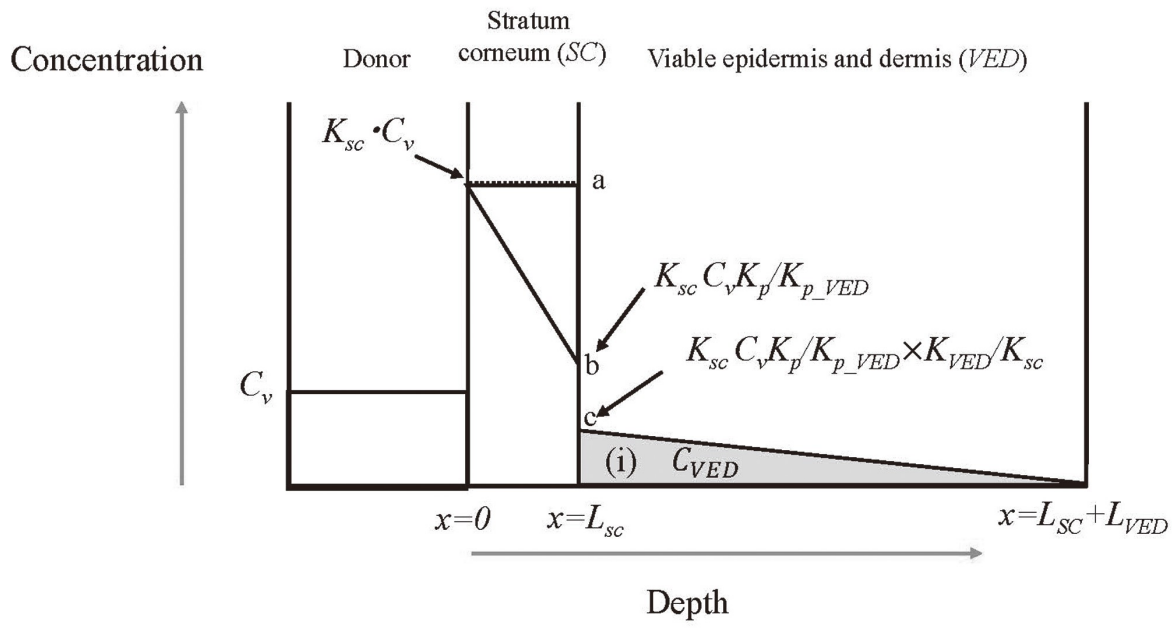

Fig. 1. Schematic diagram of concentration-distance profile in two-layered models in membrane permeation experiments. C_v: Donor concentration, K_{SC}: Partition coefficient of chemical into the *SC*, K_{VED}: Partition coefficient of chemical into the *VED*, K_p: Permeability coefficient of chemical through full-thickness skin, K_{P_VED}: Permeability coefficient of chemical through the *VED*, L_{SC}: Thickness of the *SC*, L_{VED}: Thickness of the *VED*, and C_{VED}: average concentration of a chemical in the *VED*. $1/K_p$ and $1/K_{P\_VED}$ are expressed with a skin resistance model with R and R_{VED}, respectively. The ratio of the line segment ab against bc at x=*L*sc should be the ratio of R_{SC} against R_{VED}.

Therefore, differences between the R_{VED}/R (K_p/K_{p_VED}) ratio in the 3D skin model and human skin may result in a large difference in the skin concentration between both membranes. Many reports have been published on the difference in K_p values and higher skin permeation through 3D skin models than human skin (Vávrová *et al*., 2014; Kano *et al*., 2010; Régnier *et al*., 1992). However, few reports have investigated skin concentration differences and R_{VED}/R ratio between 3D skin model and human skin.

It is important to realize that skin metabolism also affects the skin concentration of the applied chemicals, such as ester compounds. Detection of mRNA, protein, and the activity of phase I metabolizing enzymes has been evaluated in 3D skin models (Hu *et al*., 2010; Götz *et al*., 2012). The skin concentration of a chemical and its metabolites is expressed using Fick's second law of diffusion incorporating the Michaelis–Menten equation in the *VED* (Sugibayashi *et al*., 1996). Therefore, metabolic parameters such as the Michaelis constant (K_m) and the maximum metabolic rate (V_{max}) as well as the R_{VED}/R ratio affect the skin concentration of a chemical and its metabolites. When the metabolites act in the cutaneous tissues, there is a possibility that the effect will be underestimated.

False-positive and -negative reactions are sometimes observed when skin irritation and acute toxicity are evaluated using 3D model models (Spielmann *et al*., 2007; Kandárová *et al*., 2006). This might be related to the skin concentration of the applied chemical and/or its metabolite in 3D skin models. In our previous report, EpiDerm 606X showed a good relationship with the K_p values of chemicals obtained from excised human skin (Kano *et al*., 2010; Sekiguchi *et al*., 2023). Thus, in the present study, EpiDerm 606X was selected as a 3D model, and the skin concentration difference compared with real skin was investigated based on a skin resistance model. In addition, the skin concentration of chemicals and their metabolites produced by carboxylesterase was also evaluated.

MATERIALS AND METHODS

Materials

Flurbiprofen (FP) was kindly provided by Lead Chemical (Toyama, Japan), antipyrine (ANP) was purchased from Fujifilm Wako Pure Chemical Corp. (Osaka, Japan), and ethyl nicotinate (EN) and nicotinic acid (NA) were purchased from Tokyo Kasei Kogyo Co., Ltd (Tokyo, Japan). Hexyl salicylate (HS) was purchased from Sigma Aldrich (St. Louis, MO, USA). Salicylic acid (SA) was purchased from Kanto Chemical Co. Inc. (Tokyo, Japan). EpiDerm™ Epi606X (EpiDerm) was purchased from Kurabo Industries Ltd. (Osaka, Japan). Other reagents and solvents were used without further purification. Table 1 shows the *M.W.* and calculated log $K_{o/w}$ (XlogP) values of chemicals obtained from Pubchem. The XlogP value was used as a parameter for the lipophilicity of the chemicals in the present study because it correlates well with log $K_{o/w}$ at pH 7.4 (Marczak *et al*., 2015).

Table 1. Molecular weight and Xlog*P* of model chemicals used in the present study.

Model chemical	*M.W.*	XlogP
FP	224.27	2.17
ANP	188.23	-1.51
EN	141.11	1.32
NA	123.11	0.36
HS	222.29	5.50
SA	138.12	2.19

Animals

Male hairless rats (WBN/ILA-Ht strain, weight 200-240 g) were purchased from the Josai University Life Science Research Center (Sakado, Saitama, Japan) or Ishikawa Laboratory Animals (Fukaya, Saitama, Japan). Hairless rats were kept in a room regulated at 25 ± 2°C with a light/dark cycle (on, off time: 9:00-21:00) repeated every 12 hours. Water and food (MF, Oriental Yeast Co., Ltd., Tokyo, Japan) were provided *ad libitum*. Animal care and experiments were conducted in accordance with the Josai University Laboratory Animal Regulations after obtaining approval from the Josai University Animal Experiment Control Committee (H24003).

In vitro skin permeation study

The abdomens of hairless rats were shaved under triple anesthesia (medetomidine hydrochloride, 0.2 mg/kg; midazolam, 2 mg/kg; butorphanol tartrate, 2.5 mg/kg, *i.p.*), the skin was removed, and the fat on the dermal side was carefully removed with scissors. Stripped skin was also obtained by stripping the *SC* off 20-times with adhesive tape (Cellotape®, Nichiban Corporation, Tokyo, Japan). Then, intact skin (skin without the stripping procedure) or stripped skin was placed between side-by-side diffusion cells (effective diffusion area, 0.95 cm^2), and phosphate-buffered saline (PBS; pH 7.4) was applied to the donor (*SC* side) and receiver cells (2.5 mL each) and allowed to hydrate the skin for 1 hour. After this hydration procedure, PBS was removed from the donor side. A solution (2.5 mL) of various chemicals was applied to the donor cell. In the case of HS application, an undiluted solution of HS was applied to the donor cell. Samples of

0.50 mL were taken periodically from the receiver side, and then the same volume of the same solvent was added to keep the volume constant. The chemical concentration in the collected sample was determined by high-performance liquid chromatography (HPLC). Sufficient amounts of chemicals were applied to the donor compartment to maintain infinite applied dose conditions (negligible decrease in drug concentration in the donor relative to the amount permeated through the skin) during the *in vitro* skin permeation test. This gave a straight line to the skin penetration profile as long as the barrier function of the *SC* was maintained.

For *in vitro* permeation tests with EpiDerm, EpiDerm was mounted in the side-by-side diffusion cell after removing the EpiDerm pieces from the plastic insert using a knife. In addition, *SC* stripped EpiDerm (stripped EpiDerm) was obtained using the following procedure: EpiDerm was warmed at 40°C using an electrical heating device for 15 min to dry the *SC*. Then, the *SC* was physically scraped off using the metal part of a 27G needle bent into an L-shape. No tape-stripping procedure was applied to EpiDerm to remove *SC* layer. This is because EpiDerm is weak against physical force, and the process of tape stripping removes not only the *SC* layer but also the living viable epidermis beneath the *SC* layer.

The other procedure was the same as the experiment with hairless rat skin. *In vitro* skin permeation tests with stripped skin were conducted to obtain skin permeation parameters K_{P_VED} and K_{VED}. *In vitro* skin permeation tests with intact skin were performed to obtain the skin concentration at steady state. In addition, the skin permeation parameter K_P was calculated from the skin permeation-time profile.

Skin concentration

After finishing *in vitro* skin permeation tests with intact skin, the applied solution was collected, and the *SC* and dermis sides of hairless rat skin were carefully washed with PBS. Excess PBS remaining on the skin surface was removed with a Kimwipe. The chemical concentration in the *VED* was obtained after 20 applications of tape stripping of intact skin. Then, the skin area where the chemical was applied was cut with scissors, and the weight was measured. The skin was carefully minced with scissors and PBS was added. Then, the skin sample was processed using an electric homogenizer (Polytron RT 1200, Kinematica Inc., Bohemia, NY, USA) to make homogenate solutions (12,000 rpm, 5 min, 4°C). After preparation of the homogenate solution containing chemicals, 16% trichloroacetic acid solution was added and stirred for 15 min, and the concentration of chemicals in the supernatant after centrifugation (15,000 rpm, 5 min, 4°C) was determined by HPLC.

Similarly, the *in vitro* permeation experiments were performed with EpiDerm, its surface was washed with PBS, and excess PBS was removed with a Kimwipe. Then, the supporting polycarbonate membrane attached to the bottom side of EpiDerm was removed. The chemical concentration in the *VED* was investigated after removal of the *SC* with tweezers physically from the tissue. The same procedures were applied for the subsequent treatments as for hairless rat skin.

The extraction ratio of each chemical was also measured with hairless rat skin and EpiDerm. The chemical solution was added to the skin homogenate solution prepared from the skin without chemical application and incubated for at 32°C for 1 hr. The extracted ratio was then calculated as the ratio of measured to theoretical values.

HPLC detection

Chemical concentrations in the receiver solution were determined using an HPLC system (Prominence, Shimadzu, Kyoto, Japan) equipped with a UV detector (SPA-20A; Shimadzu). The collected receiver solution sample was mixed with acetonitrile with or without an internal standard in a 1:1 volume ratio and centrifuged at 21,500 × *g* at 4°C for 5 min to remove proteins and contaminants. The obtained supernatant was injected into the HPLC system. The HPLC system consisted of a pump (LC-20AD; Shimadzu), UV detector (SPD-20A; Shimadzu), system controller (SCL-10AVp; Shimadzu), and auto injector (SIL-20A; Shimadzu). The Inertsil® ODS-3 column (4.6 × 150 mm, 3.5 µm; GL Sciences Inc., Tokyo, Japan) was maintained at 40°C during elution of acetonitrile: 0.1% phosphoric acid = 1:1 for FP, acetonitrile: 0.1% phosphoric acid = 1:1 for ANP, acetonitrile: 0.1% phosphoric acid containing 5 mM SDS = 1:2 for EN and NA, acetonitrile: 0.1% phosphoric acid = 8:2 for mobile phases at a rate of 1.0 mL/min. Peaks were detected at 254 nm for FP, ANP, HS, and SA, and at 260 nm for EN and NA. As international standards isopropyl *p*-hydroxybenzoate for FP and hexyl *p*-hydroxybenzoate for HS and SA were used. An absolute calibration method was applied for the detection of ANP, EN, and NA.

Skin permeation parameters

The cumulative amount of the skin permeation of chemicals at time *n*, Q_n was calculated using the following equation (6).

$$Q_n = \left(C_n \times V_r + \sum_{i=1}^{n-1} C_i \times V_s\right)/A. \quad (6)$$

where C_n is the concentration of chemicals in the sample, V_r is the receiver volume of the diffusion cell, $\sum_{i=1}^{n-1} C_i$ is the sum of the concentrations of chemicals in the sampling solution, *Vs* is the sample volume, and *A* is the effective skin permeation area (1.77 cm^2). The steady-state flux, J_{ss}, is expressed as the slope of the linear portion of the obtained permeation profile by regression analysis with at least three successive points. The J_{ss} is also expressed using the following equation (7):

$$J_{ss} = \frac{C_v \cdot D \cdot K}{L} = C_v \cdot K_p \quad (7)$$

where K_p is further expressed as the product of partition parameter (*KL*) and diffusion parameter (D/L^2). The lag time, t_{lag} was calculated as the intersection of the extrapolation of the linear steady-state skin permeation profile with the time axis. t_{lag} is expressed with *D* and *L* using the following equation (8):

$$t_{lag} = \frac{L^2}{6D} \quad (8)$$

When the skin permeation test with a full-thickness skin was conducted, K_p was calculated from the average J_{ss} obtained from the permeation profile. On the other hand, in the skin permeation test performed with *SC* stripped skin, K_{p_VDE}, D_{VED}, and K_{VED} were calculated from the average J_{ss} obtained from the average permeation profile. The permeation parameters K_p and K_{p_VED} were obtained from three to four repeated experiments, and the permeation parameters K_{p_VED} and D_{VED} in EpiDerm and rat skin were estimated from the average skin permeation profile, and EpiDerm (53 μm) (Kano *et al.*, 2011) and rat skin (580 μm) (Kano *et al.*, 2011) were set to the *L* values of *VED* thickness, respectively. In addition, chemical concentrations of ANP and FP in *VED* were calculated with the following equation with the obtained permeation parameters (9) (Sugibayashi *et al.*, 2010):

$$C_{VED} = \frac{K_{VED} \cdot C_v \cdot K_p \Big/ K_{p\_VED}}{2} \quad (9)$$

RESULTS

Figure 2 shows the permeation profiles of ANP, a hydrophilic chemical, through hairless rat skin and EpiDerm. The permeation of ANP through *SC*-stripped skin (Fig. 2b and d) was found to be higher in both skins compared with those through full-thickness skin (Fig. 2a and c). When Q_{4h} values through full-thickness skin were compared between hairless rat skin and EpiDerm, the Q_{4h} value through EpiDerm (Fig. 2c) was higher than that through hairless rat skin (Fig. 2a). On the other hand, the Q_{30min} value through hairless rat was higher through the *SC*-stripped skin than that through EpiDerm. Notably, there was a large difference in Q_{30min} values in hairless rat skin through full-thickness and *SC*-stripped skins, but a slightly higher Q_{4h} values were confirmed in *SC*-stripped EpiDerm (Fig. 2d) compared with through full-thickness EpiDerm (Fig. 2c).

Figure 3 shows the permeation profiles of FP, a lipophilic chemical, through hairless rat skin and EpiDerm. The same tendency for the FP permeation was observed as like in the ANP permeation, such as a slightly higher permeation through *SC*-stripped EpiDerm (Fig. 3d) than through corresponding full-thickness skin (Fig. 3c). Table 2 summarizes the permeation parameters obtained from the permeation profiles of ANP and FP. The K_p and K_{P_VED} values observed with FP application were higher than those observed with ANP application. However, the K_{p_VED} values in EpiDerm were lower than those observed in hairless rat skin, although the calculated K_{VED} values were almost the same between them when the same chemical was applied. Then, K_p / K_{p_VED} or $R_{\_VED}/R_{\_}$ was calculated for hairless rat skin and EpiDerm. The $R_{\_VED}/R$ values of ANP in hairless rat skin and in EpiDerm were 1.8×10^{-3} and 6.1×10^{-1}, respectively, and the $R_{\_VED}/R$ values of FP in hairless rat skin and in EpiDerm were 2.4×10^{-2} and 7.7×10^{-1}, respectively.

Table 3 shows the steady-state *VED* concentrations of ANP and FP obtained from the *in vitro* skin permeation tests. After finishing the experiment with full-thickness skin, the *VED* concentration was obtained after removal of the *SC* using the tape-stripping method. *VED* concentrations in EpiDerm were higher than those in hairless rat skin for both ANP and FP applications. The calculated *VED* concentrations in hairless rat skin and EpiDerm exhibited differences, except for ANP in hairless rat skin, where the difference was within a 2-fold range.

Figure 4 shows the permeation profiles of ester compound EN and its metabolite NA through hairless rat skin and EpiDerm after the application of EN. When EN was applied to hairless rat skin, the Q_{6h} value of NA was higher than that of EN (Fig. 4a). However, the results were the opposite when EN was applied to EpiDerm (Fig. 4b). NA permeation was confirmed in EpiDerm, but the Q_{1h} value for NA was much lower than that for EN.

Figure 5 shows the permeation profiles of ester com-

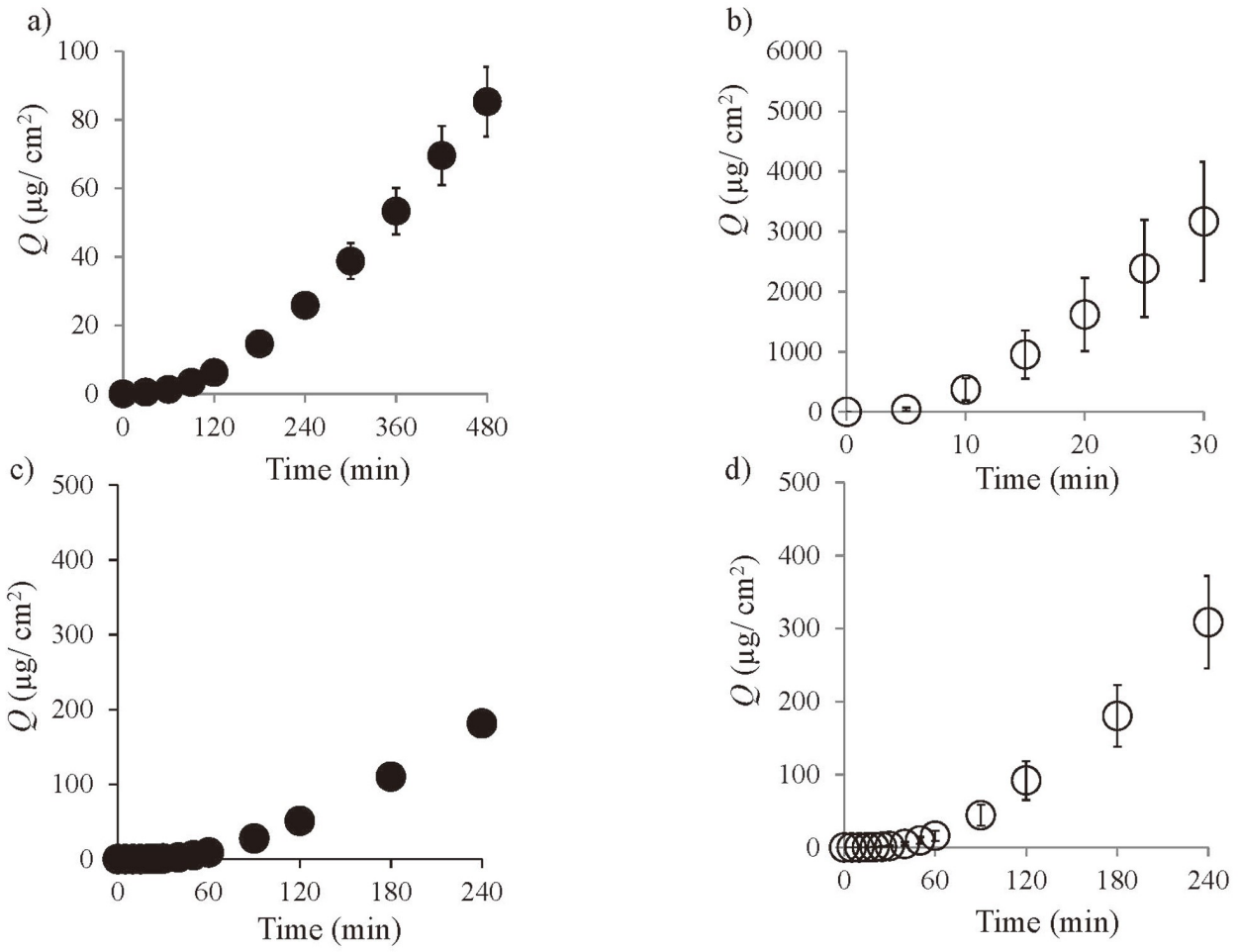

Fig. 2. Cumulative amount of antipyrine (*Q*) that permeated through hairless rat skin (a, b) and EpiDerm (c, d). Symbols: closed circle: full-thickness skin, and open circle: *SC*-removed skin. Mean ± S.E. (n=4).

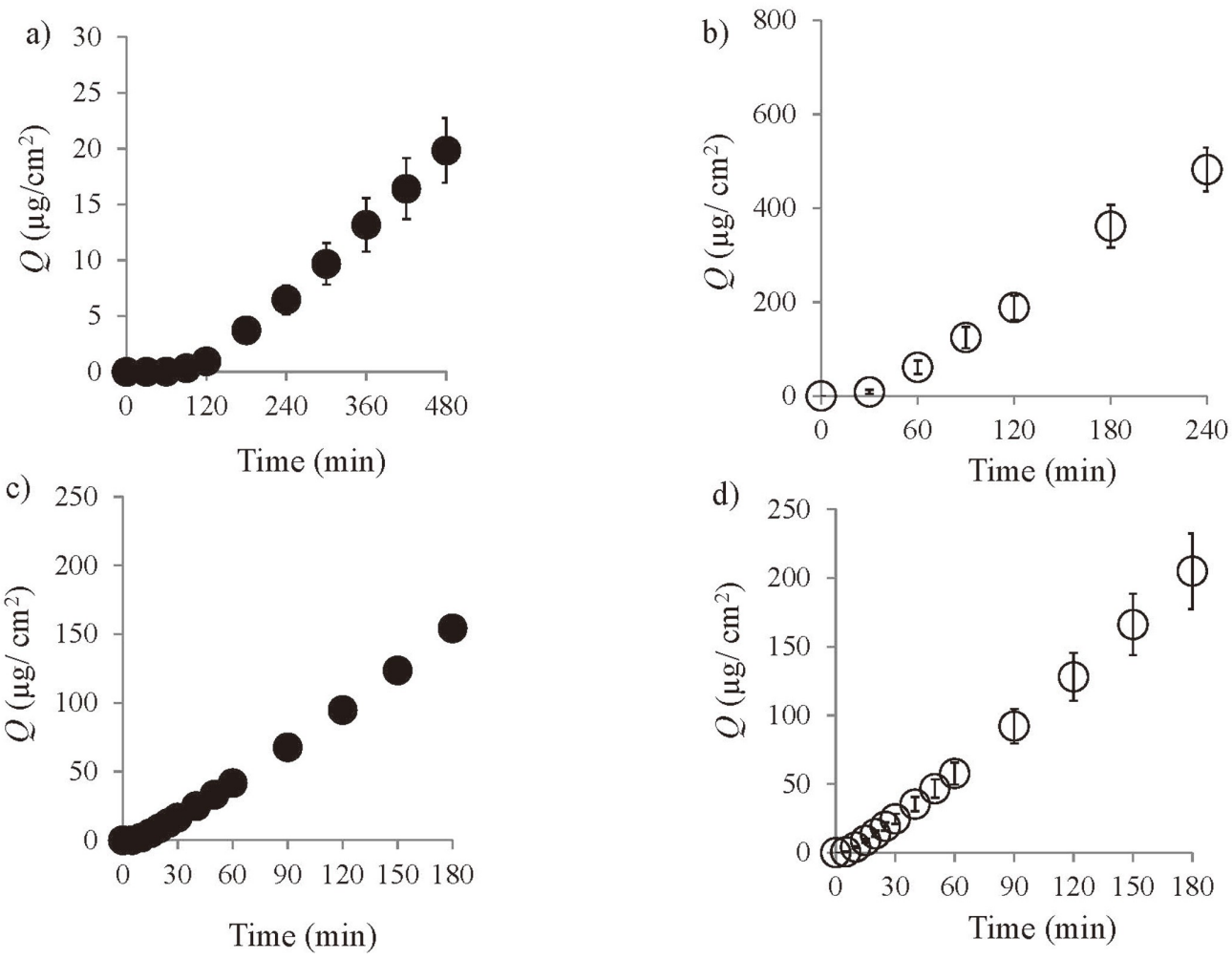

Fig. 3. Cumulative amount of flurbiprofen (*Q*) that permeated flurbiprofen through hairless rat skin (a, b) and EpiDerm (c, d). Symbols: closed circle: full-thickness skin, and open circle: *SC*-removed skin. Mean ± S.E. (n=3-4).

Chemical concentration in 3D skin model after topical application

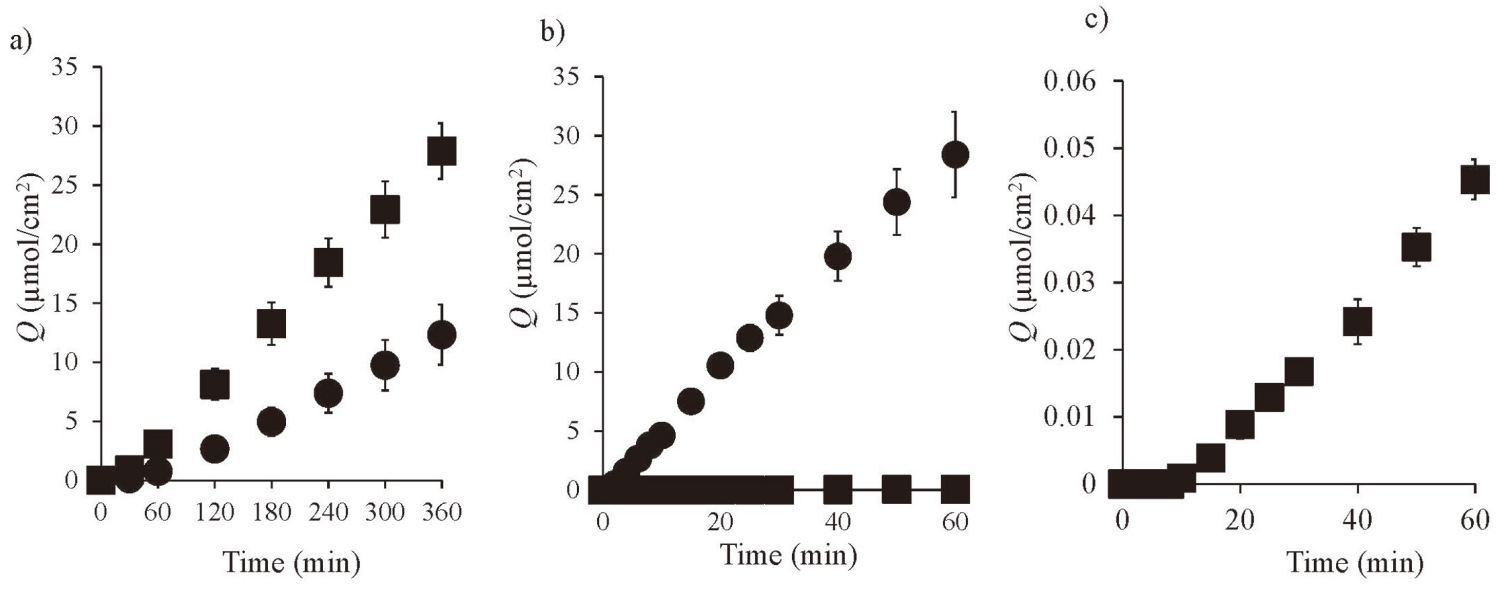

Fig. 4. Cumulative amount of nicotinate and nicotinic acid (Q) that permeated through full-thickness hairless rat skin (a) and EpiDerm (b, c) after application of ethyl nicotinate. Symbols: ●: ethyl nicotinate, and ■: nicotinic acid. c) Enlarged y-axis of (b) with respect to the permeation of NA. Mean ± S.E. (n=3-4).

Table 2. Skin permeation parameters after topical application of ANP and FP.

Applied chemical	Applied conc.	Hairless rat skin			EpiDerm		
		Full-thickness skin (cm/s)	*SC*-stripped skin (cm/s)	K_{VED}	Full-thickness skin (cm/s)	*SC*-stripped skin (cm/s)	K_{VED}
ANP	0.71 g/mL	$(5.29 \pm 0.62)\times10^{-9}$	$(2.29 \pm 0.37)\times10^{-6}$	0.17	$(3.76 \pm 0.25)\times10^{-8}$	$(6.20 \pm 0.47)\times10^{-8}$	0.11
FP	3.46 μg/mL	$(3.59 \pm 0.40)\times10^{-7}$	$(1.49 \pm 0.13)\times10^{-5}$	4.4	$(4.63 \pm 0.21)\times10^{-6}$	$(6.04 \pm 0.81)\times10^{-6}$	3.2

Table 3. Concentrations of ANP and FP in hairless rat skin and EpiDerm after topical application.

	Hairless rat skin		EpiDerm	
Applied chemical	Observed C_{VED} (mg/mL)	Calculated C_{VED} (mg/mL)	Observed C_{VED} (mg/mL)	Calculated C_{VED} (mg/mL)
ANP	0.50 ± 0.04	0.11	43.09 ± 16.14	23.7
FP	0.45 ± 0.00	0.25	6.79 ± 0.08	3.99

C_{VED}: concentration in the viable skin after stripping off the *SC* layers. Values are the mean ± S.E. (n=4).

Table 4. Concentrations of EN, HS, and their metabolites in the viable epidermis and dermis of hairless rat skin and EpiDerm.

	Hairless rat skin C_{VED} (μmol/mL)	EpiDerm C_{VED} (μmol/mL)
EN	15.61 ± 2.69	46.52 ± 4.75
NA	20.42 ± 0.94	1.02 ± 0.02
HS	1.90 ± 0.01	16.28 ± 4.99
SA	0.25 ± 0.00	0.69 ± 0.05

C_{VED}: concentration in the viable skin after stripping off the *SC* layers. Values are the mean ± S.E. (n=4).

pound HS and its metabolite SA through hairless rat skin and EpiDerm after the application of HS. In contrast to the application of EN, skin permeation of HS was not detected even in hairless rat skin until 8 hr after application, and only the permeation of metabolite SA was confirmed in hairless rat skin as well as in EpiDerm. When Q_{8h} values with SA were compared between hairless rat skin as well as in EpiDerm, EpiDerm showed a higher skin permeation than hairless rat skin.

Table 4 shows the steady state skin concentration of EN, HS, and their metabolites in hairless rat skin and EpiDerm. The *VED* concentrations of the parent compounds EN and HS in EpiDerm were higher than those in hairless rat skin. On the other hand, the *VED* concentration of the metabolite NA was lower in EpiDerm than in hairless rat skin, although the *VED* concentration of SA was higher in EpiDerm than that in hairless rat skin.

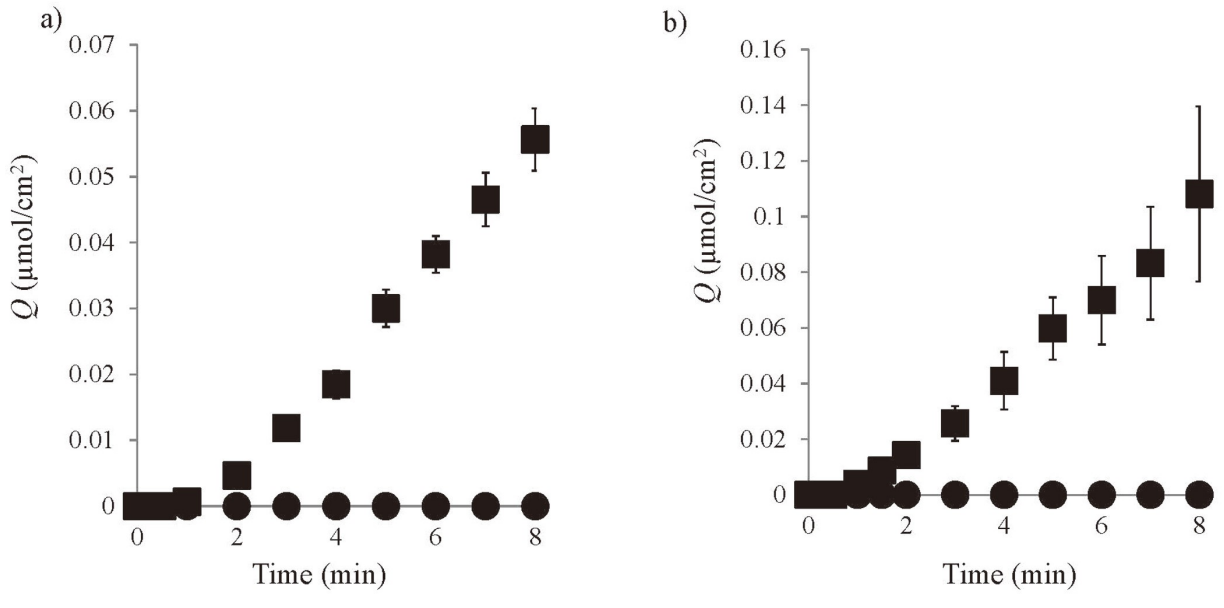

Fig. 5. Cumulative amount of hexyl salicylate and salicylic acid (Q) that permeated through full-thickness hairless rat skin (a) and EpiDerm (b) after the application of hexyl salicylate. Symbols: ●: hexyl salicylate, and ■: salicylic acid. Mean ± S.E. (n=3-4).

DISCUSSION

Differences in the *SC* lipid composition such as ceramides and fatty acids and their organization between native human skin and 3R skin models may be the main reason for the weaker barrier function of the 3R skin model than human skin (SCCS, 2010; Ponec *et al*., 2000; Vávrová *et al*., 2014). The skin concentration of topically applied chemicals is strongly related to their skin permeation rates (Kretsos *et al*., 2004; Sugibayashi *et al*., 2010; Scheuplein, 1967). When the skin was assumed to be a single membrane, the steady-state skin concentration of an applied chemical is expressed as K·Cv/2 (Herkenne *et al*., 2007). In addition, Hatanaka *et al*. (2015) reported that skin the concentration after topical application of chemicals can be accurately estimated with skin permeation parameters. Therefore, the obtained skin concentration should be theoretically identical when the K value in 3D skin models was the same as in native skin. Sugibayashi *et al*. (2010) reported that steady-state concentrations of topically applied chemicals both in *SC* and *VED* were estimated with skin permeation parameters, *i.e*., K_{ved} and K_{P_VED}. A weak barrier function of the *SC* and a higher ratio of K_p/ K_{p_VED} are the reason for the higher concentration of the applied chemicals.

The chemical concentration in the *VED* is very important because topically applied pharmaceuticals and cosmetics must be assessed for their skin toxicities. 3D skin models have been widely used to evaluate acute skin irritation (Filaire *et al*., 2022; Zhao *et al*., 2023), skin brightening, and anti-aging effects (Khmaladze *et al*., 2020). In general, the tissue response at the target site is expressed using the Hill equation (Hill, 1910), which is a formula relating concentration and response. Therefore, higher and lower *VED* concentrations result in false-positives and -negatives for topically applied chemicals compared with *in vivo* results. Thus, we focused on the barrier function of the *VED* against skin permeation in the present study.

Hairless rat skin was used instead of human skin in the present study, because a good relationship was observed with K_p in hairless rat and human skin (Rougier *et al*., 1987; Neupane *et al*., 2020), although skin esterase activity varies greatly among species (Prusakiewicz *et al*., 2006; Ngawhirunpat *et al*., 2004). In the present study, $R_{\_VED}/R$, an index of the *VED* contribution to the total barrier function of the chemical permeation through the whole skin, was higher in EpiDerm for both chemicals. The remaining of *SC* layers in EpiDerm after the removal process was not confirmed in the present study, but the K_{VED} values in hairless rat skin and EpiDerm calculated from the permeation profiles were almost the same. Thus, the K_{VED} value is related to the partitioning of chemicals into the *VED*, suggesting that both skins have similar membrane characteristics, especially in the terms of membrane lipophilicity, after removal of the *SC* layer from the full-thickness skin. In addition, the calculated *VED* concentrations of ANP and FP were within two-fold differences compared with observed values, except for ANP in hairless rat skin. Generally, the predominant skin permeation route of chemical is through to the *SC* (Naik *et al*., 2000). However, for a hydrophilic chemical such as ANP (Xlog*P*: -1.5) and a high molecular weight compound, the contribution of the skin appendage route such

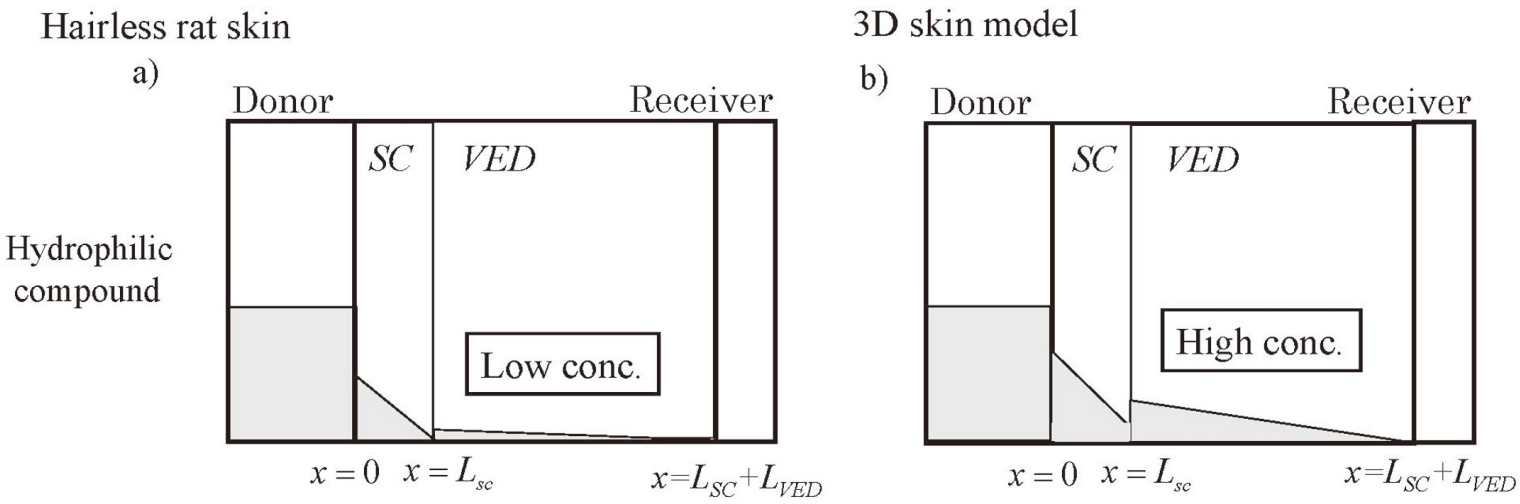

Fig. 6. Schematic diagram of the steady-state skin concentration-distance profile after application of hydrophilic (a, b) and lipophilic chemicals (c, d) using hairless rat skin (a, c) and the 3D skin model (b, d). Gray color shows the skin concentration of the applied chemicals. L_{SC}: Thickness of the *SC*, L_{VED}: Thickness of the *VED*

as hair follicles and sweat ducts against the overall skin permeation becomes important (Barry, 2002). The model to calculate *VED* concentration was constructed with chemical permeation through the *SC* route, with no consideration of involvement in the trans-appendage route. Therefore, the *VED* concentration of the hydrophilic chemical of ANP in hairless rat skin was underestimated in the present study. No investigation was conducted to evaluate detailed chemical concentration-depth profiles in the *SC* and *VED*. However, Fleischli *et al*. (2015) investigated the *in vivo* depth profile in the *SC* of applied chemicals with confocal Raman microscopy. They compared Raman signal intensity in the *SC* derived from chemicals between human skin and 3D model of SkinEthic RHE after application of caffein, salicylic acid, benzoic acid, and 4-methylbenzylidene. The Raman signal intensities in the *VED* in SkinEthic RHE were higher than those obtained in human skin. Therefore, the chemical concentration in the *VED* was assumed to increase in 3D skin, which was due to a weaker barrier function in *SC*.

Figure 6 illustrates concentration-depth profiles in the skin, considering the barrier function of the *VED* against the permeation of chemicals through whole skin. A higher *VED* concentration can be obtained due to the weak barrier function of the *SC* (Fig. 6b), suggesting that a false-positive result may be observed when evaluated with the 3D skin model.

When the ester compound EN was applied, a different behavior was observed between hairless rat skin and in EpiDerm. Species differences in ester metabolism activity have been reported (Prusakiewicz *et al*., 2006; Ngawhirunpat *et al*., 2004). Kano *et al*. (2011) reported differences in metabolite distribution in 3D skin models. Sugibayashi *et al*. (1996) proposed a mathematical model to predict the skin permeation of ester compounds by incorporation of the Michaelis-Menten equation in Fick's second law of diffusion. Then, the reason for the different skin concentrations is related to the difference in V_{max} and K_m between hairless rat skin and EpiDerm, in addition to the difference in the $R_{\_VED}/R$. Sugibayashi *et al*. (2004) reported a 30-fold higher V_{max}/K_m value in hairless rat skin compared with that in an LSE-high 3D skin model when metabolism experiments were conducted with skin homogenates. Therefore, the amount (V_{max}) and

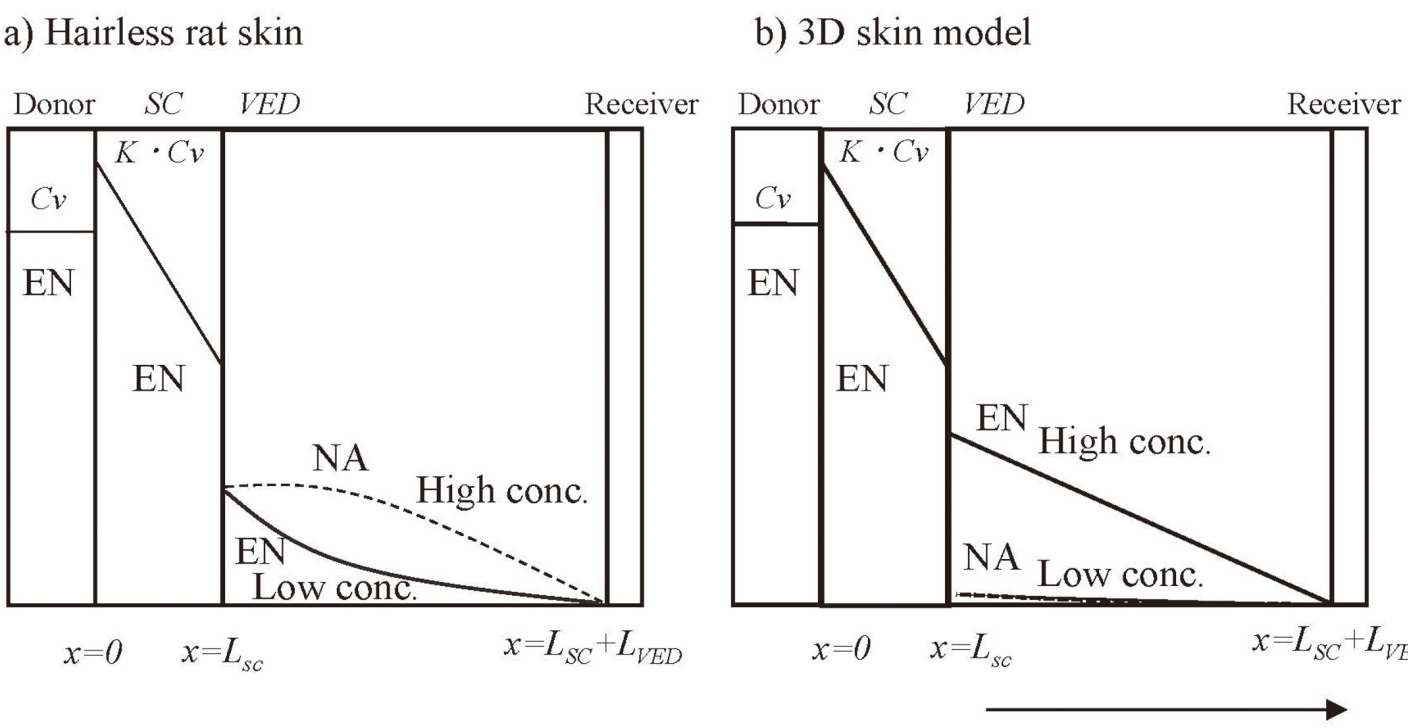

Fig. 7. Schematic diagram of the skin concentration-distance profile of ethyl nicotinate and nicotinic acid after the application of ethyl nicotinate using hairless rat skin (a) and the 3D skin model (b). Solid and dotted lines show the skin concentration of ethyl nicotinate and nicotinic acid, respectively. L_{SC}: Thickness of the *SC*, L_{VED}: Thickness of the *VED*

affinity (K_m) of enzymes should be considered when we select 3D skin models to evaluate chemicals that can be metabolized in the skin. Figure 7 shows typical concentration-distance profiles of EN and NA in hairless rat skin (Fig. 7a) and EpiDerm (Fig. 7b) after topical application of EN. According to the above assumption, a lower concentration in the *VED* may give a false-negative result when the metabolite is the cause of skin toxicity.

When HS was applied, the skin permeation of its metabolite SA was observed. *In vitro* skin permeation tests of ^{14}C-radiolabelled HS in dipropylene glycol with excised human skin results in the major component of SA and an absence of HS (ECHA, 2022). The carboxylesterase 1 (CES1) and CES2 families are the main esterases involved in the hydrolysis of many prodrugs and xenobiotics (Imai *et al*., 2016). CES1 preferentially hydrolyzes esters with a small alcohol group and a large acyl group and CES2 preferentially hydrolyzes esters with a large alcohol group (ECHA, 2022). The expression of CES family esterases in the skin is related to metabolite concentration in the *VED*. Therefore, this may be the reason for the lower *VED* concentration of SA in hairless rat skin than in EpiDerm. Further experiments using human skin and other 3D skin models should be conducted to understand the results of 3D skin models in evaluating the efficacy and toxicity of locally applied chemicals.

Conclusion

3D skin models have received increasing attention as excellent alternatives to animal testing for evaluation of the efficacy and toxicity of topically applied chemicals. Further investigation is necessary to provide experimental results on the difference in skin concentrations that affect false-positive and -negative results. However, the findings in the present study indicated that the barrier function of 3D skin models significantly affected not only skin permeation rate but also the concentration of the chemicals. Therefore, understanding the characteristics of 3D skin models is necessary for the evaluation of efficacy and toxicity of topically applied chemicals. In addition, research to improve the barrier function of 3D skin models should attract more attention.

Conflict of interest---- The authors declare that there is no conflict of interest.

REFERENCES

Barry, B.W. (2002): Drug delivery routes in skin: a novel approach. Adv. Drug Deliv. Rev., **54** (Suppl 1), S31-S40.

ECHA (2022): Committee for Risk Assessment RAC, Opinion proposing harmonised classification and labelling at EU level of Hexyl salicylate [(accessed on 12 October 2024)] https://echa.europa.eu/documents/10162/88845f59-c1f3-1302-2701-e684a9193ef7).

Filaire, E., Nachat-Kappes, R., Laporte, C., Harmand, M.F., Simon,

M. and Poinsot, C. (2022): Alternative *in vitro* models used in the main safety tests of cosmetic products and new challenges. Int. J. Cosmet. Sci., **44**, 604-613.

Fleischli, F.D., Morf, F. and Adlhart, C. (2015): Skin concentrations of topically applied substances in reconstructed human epidermis (rhe) compared with human skin using *in vivo* confocal raman microscopy. Chimia (Aarau), **69**, 147-151.

Gibbs, S., van de Sandt, J.J., Merk, H.F., Lockley, D.J., Pendlington, R.U. and Pease, C.K. (2007): Xenobiotic metabolism in human skin and 3D human skin reconstructs: a review. Curr. Drug Metab., **8**, 758-772.

Götz, C., Pfeiffer, R., Tigges, J., Blatz, V., Jäckh, C., Freytag, E.M., Fabian, E., Landsiedel, R., Merk, H.F., Krutmann, J., Edwards, R.J., Pease, C., Goebel, C., Hewitt, N. and Fritsche, E. (2012): Xenobiotic metabolism capacities of human skin in comparison with a 3D epidermis model and keratinocyte-based cell culture as *in vitro* alternatives for chemical testing: activating enzymes (Phase I). Exp. Dermatol., **21**, 358-363.

Hatanaka, T., Yoshida, S., Kadhum, W.R., Todo, H. and Sugibayashi, K. (2015): In silico estimation of skin concentration following the dermal exposure to chemicals. Pharm. Res., **32**, 3965-3974.

Herkenne, C., Naik, A., Kalia, Y.N., Hadgraft, J. and Guy, R.H. (2007): Dermatopharmacokinetic prediction of topical drug bioavailability *in vivo*. J. Invest. Dermatol., **127**, 887-894.

Hill, A.V. (1910): The possible effects of the aggregation of the molecules of haemoglobin on its dissociation curves. J. Physiol., **40**, 4-7.

Hu, T., Khambatta, Z.S., Hayden, P.J., Bolmarcich, J., Binder, R.L., Robinson, M.K., Carr, G.J., Tiesman, J.P., Jarrold, B.B., Osborne, R., Reichling, T.D., Nemeth, S.T. and Aardema, M.J. (2010): Xenobiotic metabolism gene expression in the EpiDermin vitro 3D human epidermis model compared to human skin. Toxicol. In Vitro, **24**, 1450-1463.

Imai, T., Ariyoshi, S., Ohura, K., Sawada, T. and Nakada, Y. (2016): Expression of carboxylesterase isozymes and their role in the behavior of a fexofenadine prodrug in rat skin. J. Pharm. Sci., **105**, 714-721.

Kandárová, H., Liebsch, M., Schmidt, E., Genschow, E., Traue, D., Spielmann, H., Meyer, K., Steinhoff, C., Tornier, C., De Wever, B. and Rosdy, M. (2006): Assessment of the skin irritation potential of chemicals by using the SkinEthic reconstructed human epidermal model and the common skin irritation protocol evaluated in the ECVAM skin irritation validation study. Altern. Lab. Anim., **34**, 393-406.

Kano, S., Todo, H., Sugie, K., Fujimoto, H., Nakada, K., Tokudome, Y., Hashimoto, F. and Sugibayashi K. (2010): Utilization of reconstructed cultured human skin models as an alternative skin for permeation studies of chemical compounds. AATEX, **15**, 61-70.

Kano, S., Todo, H., Furui, K., Sugie, K., Tokudome, Y., Hashimoto, F., Kojima, H. and Sugibayashi, K. (2011): Comparison of several reconstructed cultured human skin models by microscopic observation: Their usefulness as an alternative membrane for skin in drug permeation experiments. AATEX, **16**, 51-58.

Khmaladze, I., Österlund, C., Smiljanic, S., Hrapovic, N., Lafon-Kolb, V., Amini, N., Xi, L. and Fabre, S. (2020): A novel multifunctional skin care formulation with a unique blend of antipollution, brightening and antiaging active complexes. J. Cosmet. Dermatol., **19**, 1415-1425.

Kretsos, K., Kasting, G.B. and Nitsche, J.M. (2004): Distributed diffusion-clearance model for transient drug distribution within the skin. J. Pharm. Sci., **93**, 2820-2835.

Marczak, M., Okoniewska, K.M., Okoniewski, J., Grabowski, T. and Jaroszewski, J.J. (2015): Indirect relationship between lipophilicity and maximum residue limit of drugs determined for fatty tissue. Bull. Vet. Inst. Pulawy, **59**, 383-391.

Mitragotri, S., Anissimov, Y.G., Bunge, A.L., Frasch, H.F., Guy, R.H., Hadgraft, J., Kasting, G.B., Lane, M.E. and Roberts, M.S. (2011): Mathematical models of skin permeability: an overview. Int. J. Pharm., **418**, 115-129.

Naik, A., Kalia, Y.N. and Guy, R.H. (2000): Transdermal drug delivery: overcoming the skin's barrier function. Pharm. Sci. Technol. Today, **3**, 318-326.

Neupane, R., Boddu, S.H., Renukuntla, J., Babu, R.J. and Tiwari, A.K. (2020): Alternatives to biological skin in permeation studies: current trends and possibilities. Pharmaceutics, **12**, 152.

Ngawhirunpat, T., Opanasopit, P. and Prakongpan, S. (2004): Comparison of skin transport and metabolism of ethyl nicotinate in various species. Eur. J. Pharm. Biopharm., **58**, 645-651.

Pirot, F., Kalia, Y.N., Stinchcomb, A.L., Keating, G., Bunge, A. and Guy, R.H. (1997): Characterization of the permeability barrier of human skin *in vivo*. Proc. Natl. Acad. Sci. USA, **94**, 1562-1567.

Ponec, M., Boelsma, E., Weerheim, A., Mulder, A., Bouwstra, J. and Mommaas, M. (2000): Lipid and ultrastructural characterization of reconstructed skin models. Int. J. Pharm., **203**, 211-225.

Potts, R.O. and Guy, R.H. (1992): Predicting skin permeability. Pharm. Res., **9**, 663-669.

Prusakiewicz, J.J., Ackermann, C. and Voorman, R. (2006): Comparison of skin esterase activities from different species. Pharm. Res., **23**, 1517-1524.

Punt, A., Bouwmeester, H., Blaauboer, B.J., Coecke, S., Hakkert, B., Hendriks, D.F., Jennings, P., Kramer, N.I., Neuhoff, S., Masereeuw, R., Paini, A., Peijnenburg, A.A., Rooseboom, M., Shuler, M.L., Sorrell, I., Spee, B., Strikwold, M., Van der Meer, A.D., Van der Zande, M., Vinken, M., Yang, H., Bos, P.M. and Heringa, M.B. (2020): New approach methodologies (NAMs) for human-relevant biokinetics predictions. Meeting the paradigm shift in toxicology towards an animal-free chemical risk assessment. Altern. Anim. Exp., **37**, 607-622.

Régnier, M., Caron, D., Reichert, U. and Schaefer, H. (1992): Reconstructed human epidermis: a model to study *in vitro* the barrier function of the skin. Skin Pharmacol., **5**, 49-56.

Rougier, A., Lotte, C. and Maibach, H.I. (1987): The hairless rat: a relevant animal model to predict *in vivo* percutaneous absorption in humans? J. Invest. Dermatol., **88**, 577-581.

SCCS. (2010): Basic Criteria for the In Vitro Assessment of Dermal Absorption of Cosmetic Ingredients. SCCS; Brussels, Belgium. [(accessed on 12 October 2024)]. pp. 1–14. Available online: https://op.europa.eu/en/publication-detail/-/publication/91793089-8206-4975-a6c9-078770655851 [Google Scholar]

Scheuplein, R.J. (1967): Mechanism of percutaneous absorption. II. Transient diffusion and the relative importance of various routes of skin penetration. J. Invest. Dermatol., **48**, 79-88.

Sekiguchi, S., Narita, I., Itakura, S., Kojima, H., Sugibayashi, K. and Todo, H. (2023): Evaluation of skin permeation order of cosmetic active compounds from commercially available cosmetic products with different dosage forms using a three-dimensional cultured human skin model. J. Jpn. Cosmet. Sci. Soc, **47**, 176-182.

Spielmann, H., Hoffmann, S., Liebsch, M., Botham, P., Fentem, J.H., Eskes, C., Roguet, R., Cotovio, J., Cole, T., Worth, A., Heylings, J., Jones, P., Robles, C., Kandárová, H., Gamer,

A., Remmele, M., Curren, R., Raabe, H., Cockshott, A., Gerner, I. and Zuang, V. (2007): The ECVAM international validation study on *in vitro* tests for acute skin irritation: report on the validity of the EPISKIN and EpiDerm assays and on the Skin Integrity Function Test. Altern. Lab. Anim., **35**, 559-601.

Stucki, A.O., Barton-Maclaren, T.S., Bhuller, Y., Henriquez, J.E., Henry, T.R., Hirn, C., Miller-Holt, J., Nagy, E.G., Perron, M.M., Ratzlaff, D.E., Stedeford, T.J. and Clippinger, A.J. (2022): Use of new approach methodologies (NAMs) to meet regulatory requirements for the assessment of industrial chemicals and pesticides for effects on human health. Front. Toxicol., **4**, 964553.

Sugibayashi, K., Hayashi, T., Hatanaka, T., Ogihara, M. and Morimoto, Y. (1996): Analysis of simultaneous transport and metabolism of ethyl nicotinate in hairless rat skin. Pharm. Res., **13**, 855-860.

Sugibayashi, K., Hayashi, T., Matsumoto, K. and Hasegawa, T. (2004): Utility of a three-dimensional cultured human skin model as a tool to evaluate the simultaneous diffusion and metabolism of ethyl nicotinate in skin. Drug Metab. Pharmacokinet., **19**, 352-362.

Sugibayashi, K., Todo, H., Oshizaka, T. and Owada, Y. (2010): Mathematical model to predict skin concentration of drugs: toward utilization of silicone membrane to predict skin concentration of drugs as an animal testing alternative. Pharm. Res., **27**, 134-142.

Takeuchi, H., Ishida, M., Furuya, A., Todo, H., Urano, H. and Sugibayashi, K. (2012): Influence of skin thickness on the *in vitro* permeabilities of drugs through Sprague-Dawley rat or Yucatan micropig skin. Biol. Pharm. Bull., **35**, 192-202.

Vávrová, K., Henkes, D., Strüver, K., Sochorová, M., Školová, B., Witting, M.Y., Friess, W., Schreml, S., Meier, R.J., Schäfer-Korting, M., Fluhr, J.W. and Küchler, S. (2014): Filaggrin deficiency leads to impaired lipid profile and altered acidification pathways in a 3D skin construct. J. Invest. Dermatol., **134**, 746-753.

Yamaguchi, K., Mitsui, T., Aso, Y. and Sugibayashi, K. (2008): Structure-permeability relationship analysis of the permeation barrier properties of the stratum corneum and viable epidermis/dermis of rat skin. J. Pharm. Sci., **97**, 4391-4403.

Zhao, H., Chen, Z., Kang, X., Yang, B., Luo, P., Li, H. and He, Q. (2023): The frontline of alternatives to animal testing: novel *in vitro* skin model application in drug development and evaluation. Toxicol. Sci., **196**, 152-169.